Mapping of Contralateral Space in Retinotopic Coordinates by a Parietal Cortical Area in Humans

M. I. Sereno,[1]* S. Pitzalis,[1]† A. Martinez,[2]‡

The internal organization of a higher level visual area in the human parietal cortex was mapped. Functional magnetic resonance images were acquired while the polar angle of a peripheral target for a delayed saccade was gradually changed. A region in the superior parietal cortex showed robust retinotopic mapping of the remembered target angle. The map reversed when the direction of rotation of the remembered targets was reversed and persisted unchanged when study participants detected rare target reappearances while maintaining fixation, or when the eccentricity of successive remembered targets was unpredictable. This region may correspond to the lateral intraparietal area in macaque monkeys.

The neocortex of each hemisphere in primates consists of a mosaic of nearly 100 visual, auditory, somatosensory, motor, and limbic areas. To precisely define their borders, studies in nonhuman primates have combined intensive microelectrode mapping, tracer injections, histological stains, and functional analysis of single unit responses and have often visualized these results on unfolded representations of the cortex (*1*–*5*). Functional magnetic resonance imaging (fMRI) in combination with retinotopic mapping stimuli (*6*) and cortical surface reconstruction (*7*–*9*) have made it possible to define the borders of early visual areas with comparable precision in humans (*10*–*12*). However, these methods have so far proved less useful in higher visual areas, which have instead been defined almost solely by their responses during different cognitive tasks. The borders of many higher visual areas in humans have yet to be precisely defined.

Studies of brain-lesioned humans have long implicated the parietal cortex in spatial processing (*13*, *14*). This has been confirmed by recent neuroimaging studies (*15*–*21*). Single-neuron recordings in awake behaving macaques suggest that parietal cortical neurons code and update target locations in retinocentric coordinates (*22*–*26*). It is less clear, however, whether remembered locations in contralateral visual space are systematically arrayed across subregions of the cortex. Some higher level areas in nonhuman primates are known to contain systematic maps of more complex stimulus features. For example, despite being insensitive to the exact retinal position of a face, small regions of the inferotemporal cortex appear to code for a sequence of orientations of the face (profile, three-quarters, and frontal) at a sequence of nearby cortical locations (*27*).

Study participants (n = 12) viewed stimuli projected onto a screen at their chin level via a mirror adjusted so that central fixation was comfortable (*28*). In the first task, participants made delayed saccades (Fig. 1, top) (*29*). A brief peripheral target was presented while participants fixated a central point. A ring of target-sized blinking distractors near the target eccentricity then appeared during a 3-s delay period while participants maintained fixation. At fixation dimming (or offset) (*30*) and distractor offset, participants made a saccade from the fixation point to the remembered target location on a black screen. Then they immediately made a saccade back to the fixation point, which brightened (or reappeared) in preparation for the next peripheral target. The time between successive target onsets was 5 s.

The angle of the remembered target location was stepped in a counterclockwise (CCW) direction through 360° so that imaging data could be analyzed with the same

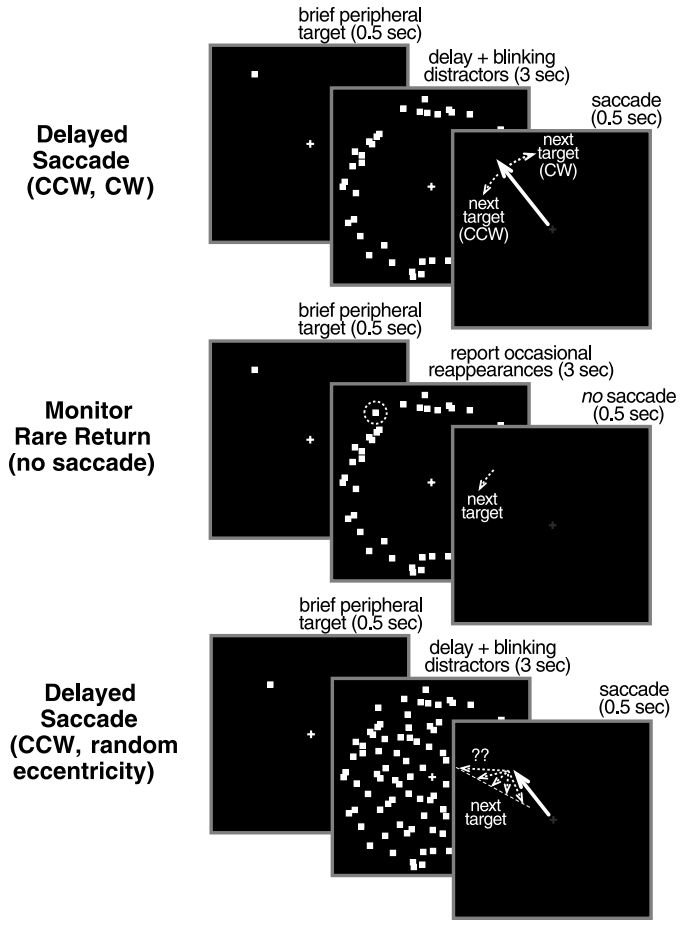

Fig. 1. Phase-encoded stimuli for generating maps of remembered location. In the first three tasks, the person is fixating centrally when a peripheral target briefly appears at 12° to 15° of eccentricity. A ring of blinking distractors appears while the person remembers the target location and maintains fixation for 3 s. In the first and second tasks (top), the person saccades to the remembered location after the delay period and then immediately saccades back to the fixation point to prepare for the next target, which appears CCW (or CW) to the last. In the third task (middle), participants merely detect when the target occasionally reappears among the distractors (it reappears on average once every 12 targets) and make no saccades. The fourth task (bottom) is similar to the first except that the eccentricity of each target is completely unpredictable (3° to 15°) and the distractors fill the entire field. In every case, the peripheral targets cover 360° of polar angle in 64 s.

[1]Department of Cognitive Science, [2]Department of Radiology, University of California, San Diego, La Jolla, CA 92093-0515, USA.

*To whom correspondence should be addressed. E-mail: sereno@cogsci.ucsd.edu

†Present address: Laboratory of Functional Neuroimaging, Fondazione Santa Lucia, Instituto di Ricovero e Cura a Carattere Scientifico, Rome, Italy.

‡Present address: Sackler Institute, Weill Medical College of Cornell University, New York, NY, USA.

Fourier-based method used to map polar angle in retinotopic visual areas (*10*). The targets were jittered slightly in eccentricity and polar angle (2.5° visual angle, both axes) to make them somewhat less predictable. One complete polar angle cycle took 64 s, so the average step in polar angle to the next target was about 28°.

Three additional versions of the task were then used to control for artifacts. In the second task (Fig. 1, top), successive targets appeared in a clockwise (CW) instead of a CCW direction. In the third task (Fig. 1, middle), participants had to detect the occasional reappearance ($P = 0.08$) of CCW-progressing targets among the flashing distractors while maintaining central fixation; in this task, they made no saccades during the entire scan. The fourth task (Fig. 1, bottom) was like the first except that the eccentricity of the next target was completely unpredictable, and the distractors filled the field.

Each functional session included a series of surface-coil echo-planar scans ($3 \times 3 \times 4$ mm voxels, 128 images per slice) focused on occipital and parietal visual areas and a single high-resolution alignment scan, which was used to register the functional data with a cortical surface reconstruction made from head-coil structural scans taken in a separate session (*31*).

Figure 2 shows the regions in the right hemisphere of one person that were activated in a periodic fashion by our phase-encoded delayed saccade task. The center of the parietal focus (the yellow cross) is shown in slice view at the bottom of the figure. Color saturation indicates the strength of the response, whereas the hue indicates the response phase. Phase-encoded mapping experiments such as this one reveal activity only in areas that have some kind of map of the encoded stimulus feature. Thus, areas activated by every target or by every saccade will not appear. Areas merely activated by every contralateral target or saccade, by contrast, will appear but show no spread in the phase angle of their response.

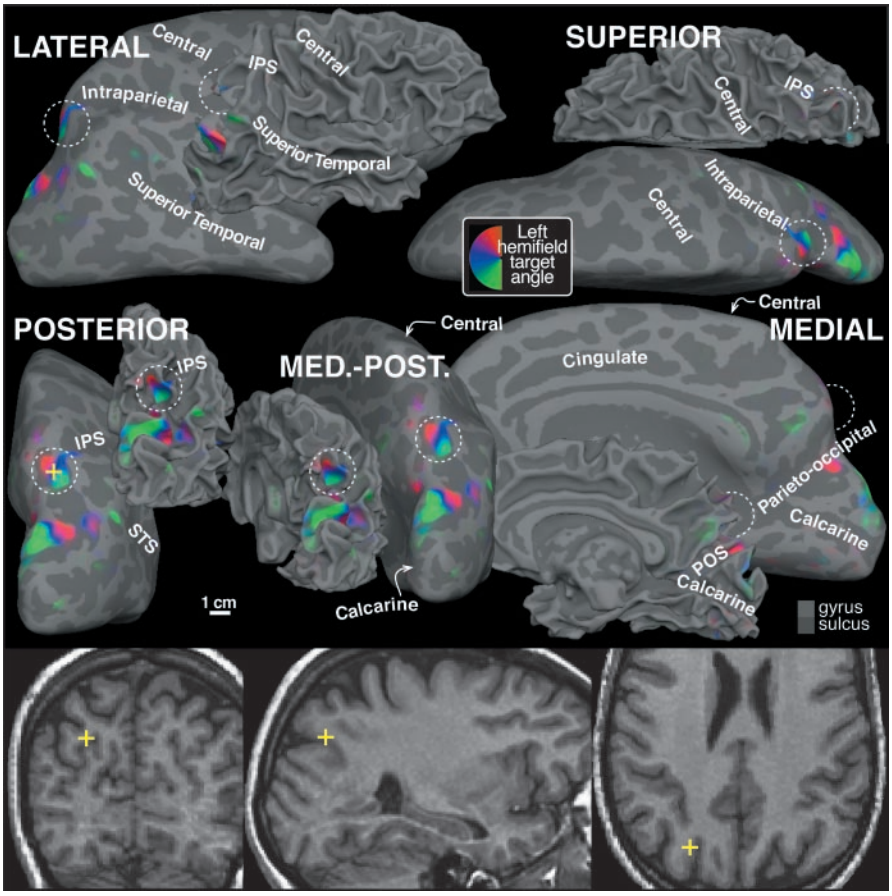

Fig. 2. Superior parietal cortical area with a map of remembered location (dotted circles). The folded and unfolded right hemisphere of a single person is shown in superior, lateral, medial, medial-posterior, and posterior views. The main sulci (dark gray) have text labels. IPS, intraparietal sulcus; STS, superior temporal sulcus; POS, parieto-occipital sulcus. The small region indicated by the dotted circles is just beyond the extreme medial tip of the intraparietal sulcus. It has a strong periodic response to the first task and a clear map of contralateral remembered targets (red, upper left visual field; blue, left horizontal; green, lower left). The map is best appreciated in the unfolded medial-posterior unfolded view (middle). The Fourier-based analysis method only reveals areas that respond differently to different target angles; thus, areas activated by all targets or all saccades will be subtracted out. The center of the parietal map (the yellow cross in the unfolded posterior view at middle left) is also marked in the three slice views at the bottom (Talairach coordinates: $x = 32$, $y = -68$, $z = 46$).

A small region of the right superior parietal cortex (dotted circle), just beyond the medial end of the intraparietal sulcus, showed the most robust retinotopic mapping of the angle of the remembered contralateral (left hemifield) targets. Lower field targets (green) were represented most inferiorly; horizontal targets were represented intermediately (blue); and upper field targets were represented superiorly (red). On the unfolded cortex, superior becomes anterior because the map is located on the anterior bank of a small sulcus. The activated region is well anterior to the superior terminus of the parieto-occipital sulcus and is slightly closer to the central sulcus than to the occipital pole (*32*). In the left hemisphere (not shown in this figure), there was a similar area with a map of remembered right hemifield targets. That map was organized in the same way. All 12 participants showed significant periodic activity in this region bilaterally with substantial phase spreads, indicating retinotopic responses. There was some variation in the exact location and form of the parietal map across participants, but upper fields were often represented superior and anterior to lower fields. There was a second, more posterior map in both hemispheres that overlaps several previously described second order retinotopic areas.

To verify the organization of the parietal map, we tested what happened when the direction of rotation of successive targets was reversed. Targets always started at the bottom of the circle (at the 6:00 position). When they moved in a CCW direction (task 1), the right hemifield was stimulated in the first half of each cycle, and the lower right visual field was stimulated before the upper right visual field. Reversing the rotation of the targets to a CW direction (task 2) will stimulate the right hemifield only after a delay of half a cycle, and upper right visual fields will now be stimulated before lower right visual fields. Task 1 responses can therefore be used to predict task 2 responses with no free parameters.

Figure 3 (top left pair) shows the left and right hemisphere activations after the standard CCW progression of targets, but now on a flattened representation of the visual cortex made after cutting off the occipital lobe and incising the depths of the calcarine sulcus. The flat right hemisphere of this pair illustrates the same data as in Fig. 2. The white circles have been drawn in exactly the same position across conditions to aid comparison. The statistical significance of the responses (contralateral versus ipsilateral contrast) is plotted in Fig. 3, top right (*33*). The response

to contralateral targets was highly significant. Ipsilateral targets evoked only a weak response, primarily from V1 center of gaze. If these cortical maps are robust, we would expect a reversed (CW) progression of targets to elicit a half-cycle delay and a reversed phase progression. This is exactly what was found (middle left) in data taken from the same person on a different scan day. To make the comparison easier, we reversed the color map and added half a cycle of phase angle to it, so that a consistent map appears the same across the two different directions of target rotation. The similar appearance of the maps in both hemispheres across these two conditions provides strong support for the idea that this small region of the superior parietal cortex represents the angle of a remembered target in a retinotopic fashion. The maps found in the more posterior focus were similarly consistent.

Neuroimaging responses elicited by a delayed saccade task could be due to simple sensory responses, processes involved in remembering a cued location, and processes underlying the execution of saccades to the target and back. The third task—monitoring rare target reoccurrence—eliminated all overt motor output and better controlled the sensory aspects of the task. Figure 3 (middle right) shows that despite the lack of any saccades, a very similarly organized set of left and right hemisphere maps of contralateral visual space was revealed. These data were taken from the same person on a third scan day. Finally, the map of polar angle persisted when the eccentricity of the next target was unpredictable and the distractors occupied the whole field (Fig. 3, bottom left, fourth scan day). The overlay (higher magnification inset at lower right) of the outline of the maps from the four stimulus conditions shows a remarkable degree of consistency across tasks and scan days.

The parietal area that we have mapped is not strongly driven by standard retinotopic mapping stimuli, which require no peripheral attention. It is also not driven by structured motion stimuli (Fig. 3, bottom right). Structured motion stimuli instead activate several more posterior areas, including the superior end of human V3A and a small area medial to it in the parieto-occipital sulcus. These data and the scans used to define early retinotopic areas (dotted lines) were collected on a fifth scan day.

To illustrate the exact relationship between all these areas, the activation pattern for task 1 has been overlaid in Fig. 4 with a set of dotted lines representing the boundaries of other early visual areas that we were able to define in this person. The borders of V1, V2, V3, VP, V3A, and V4v were determined by mapping visual field sign (*10*). The areas responding to simple motion (from a sixth scan day) were determined by comparing moving and stationary patterns at low contrast (labeled "low contrast"). Finally, the areas responding selectively to more complex moving patterns (labeled "flow fields") were transcribed from Fig. 3.

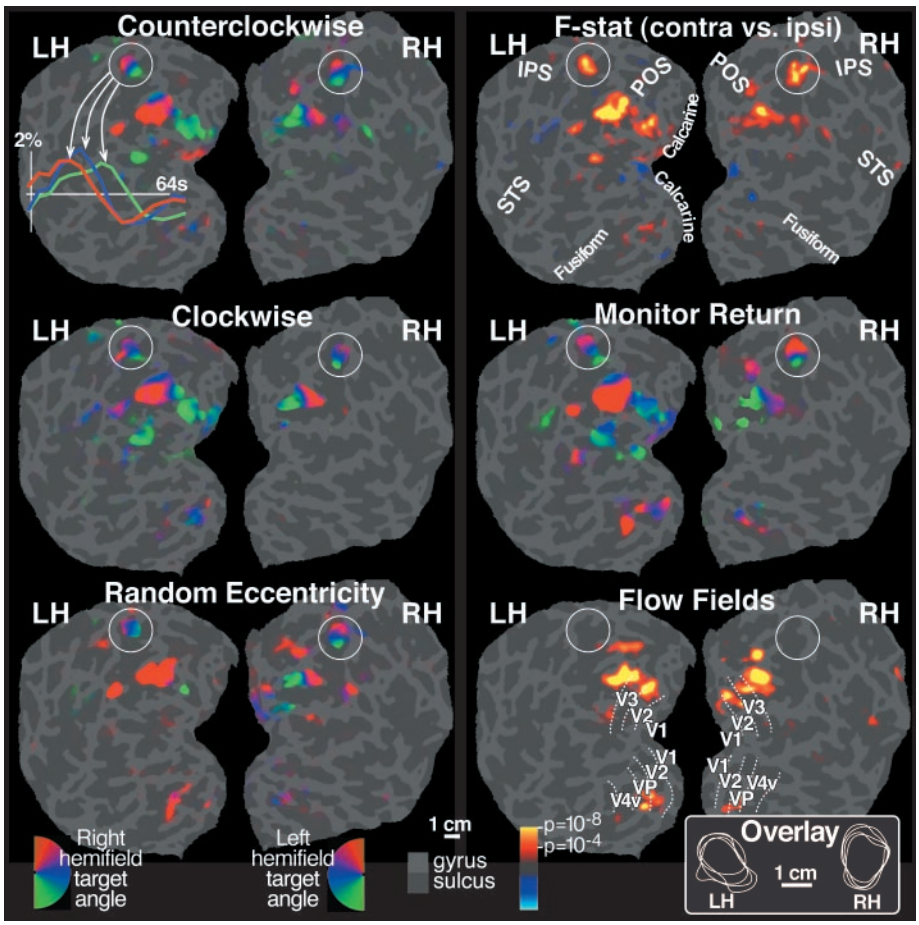

Fig. 3. The parietal cortex map (circles are in exactly equivalent positions to aid comparison) is constant across all four tasks from Fig. 1. LH, left hemisphere; RH, right hemisphere. The results of five different scan sessions on a single person are shown in six groups of flattened images. The data from Fig. 2 are shown in the top row (phase is plotted at left and significance values for contralateral versus ipsilateral are plotted at the right). Differences in the phase of the response are obvious in three individual pixel time courses plotted in the upper left inset. Changing the direction of rotation of the targets (middle left) left the map unchanged (half a cycle of phase was added to the color scale, and it was reversed so that red still indicates upper and green lower). A similar map was obtained for detection of occasional reoccurrences without saccades (middle right) and for making delayed saccades where the eccentricity of the next target was unpredictable (lower left). The last (lower right) group shows that the circled parietal area does not distinguish the difference between structured and unstructured motion (flow fields) and lies well anterior to early retinotopic areas (visual area borders were traced from retinotopic mapping data not otherwise shown).

The overlay indicates that the second more posterior map revealed by the remembered saccade tasks partly overlaps an area previously labeled V3A; and the remembered saccade map matches the polar angle map found in this area with standard retinotopic mapping stimuli (*34*). The second map is superior to the part of V3A that is strongly activated by low-contrast moving patterns and partially overlaps the more inferior of the two regions selectively driven by complex patterned moving stimuli. Given these data, it is possible that V3A as originally defined contains more than one visual area (*35*). This posterior focus has been coactivated with the parietal cortex before (*15*). Distinguishing how the two regions differ functionally (beyond their contrasting responses to passive retinotopic mapping stimuli) remains a goal for future experiments, as does determining the exact order of their activation.

The stimuli for tasks 1 through 4 do contain a small periodic retinotopic stimulus—namely, the brief peripheral target. Some of the responses we observed might have been due to this passive stimulus as opposed to the task of remembering its position. However, the lack of a significant parietal activation in experiments using standard (highly salient) retinotopic mapping stimuli and the virtual silence of V1 and V2 in our tasks make it unlikely that our large parietal activations

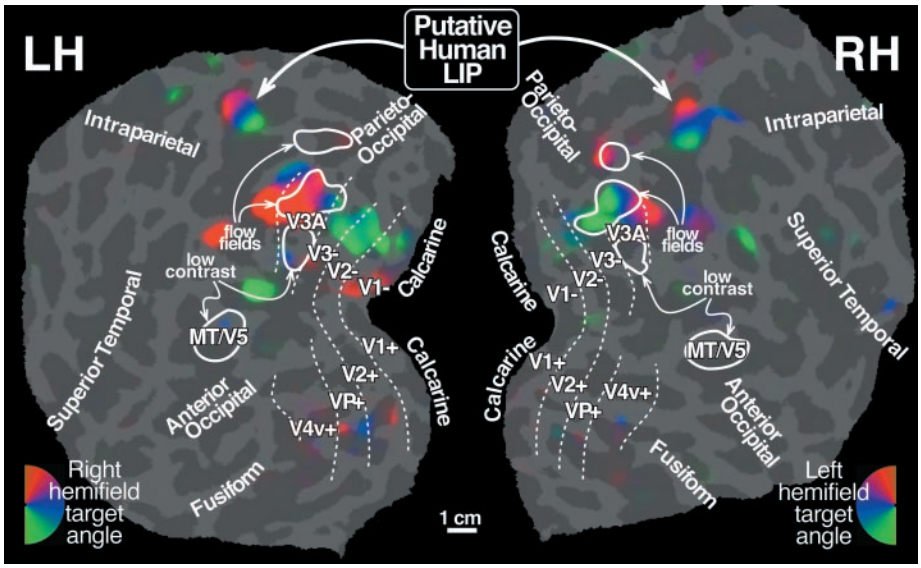

Fig. 4. Location of the putative human area LIP in relation to other visual areas. The boundaries of early visual areas are superimposed with dotted lines on the responses to the first task. The borders of V1, V2, V3, VP, V3A, and V4v were determined by means of the visual field sign method, and the borders of four motion-sensitive areas were determined by strong responses to low-contrast moving versus stationary stimuli (MT/V5 and the inferior part of V3A) and to structured versus unstructured motion stimuli (an area in the superior part of V3A and another area superior to it). The putative human LIP is situated well anterior to other retinotopic areas: about halfway between the central sulcus and the occipital pole.

were due to passive sensory responses. In contrast with the small brief target, the prominent long-lived ring of blinking distractors is likely to have strongly stimulated early retinotopic visual areas such as V1, V2, V3, and VP. The distractors, however, had no periodicity near 64 s, so this strong activation would be "subtracted out" by our analysis (*36*). Finally, previous studies manipulating visual attention with exactly equated retinotopic stimulation have demonstrated attention-related responses in early visual areas; this makes it possible that the weak responses we observed in early retinotopic areas were due as much to attention to particular visual field locations as to simple sensory responses to the brief targets (*37*).

The representation of the angle of saccade target (independent of whether a saccade is actually made) is reminiscent of data collected from single neurons in posterior parietal and prefrontal visual areas in the macaque monkey (*22–25*, *29*, *38*). This suggests that remembered targets are buffered and updated in retinotopic coordinates as the animal makes saccades to remembered targets. It is as though the animal is visualizing in retinotopic coordinates where the target would be on a retinotopic map had the target stayed on. Our results go beyond most existing parietal cortex data in suggesting that this updating might actually take place in a retinotopic map that is systematically spread across the cortex (*39*), similar to what has been seen in the superior colliculus (*40*) and also possibly in the prefrontal cortex (*29*). We think that the region we have mapped might be closely related to the lateral intraparietal area (LIP) of macaque monkeys. Interestingly, this region has also been activated in neuroimaging studies by linguistic tasks that lack any explicit requirement for remembering the location of visual targets.

References and Notes

1. J. H. Kaas, *Brain Res. Bull.* **44**, 107 (1997).
2. D. J. Felleman, D. C. Van Essen, *Cereb. Cortex* **1**, 1 (1991).
3. L. Krubitzer, *Trends Neurosci.* **18**, 408 (1995).
4. W. A. Suzuki, D. G. Amaral, *J. Neurosci.* **14**, 1856 (1994).
5. M. I. Sereno, C. T. McDonald, J. M. Allman, *Cereb. Cortex* **4**, 601 (1994).
6. S. A. Engel *et al.*, *Nature* **369**, 525 (1994).
7. A. M. Dale, M. I. Sereno, *J. Cognit. Neurosci.* **5**, 162 (1993).
8. B. Fischl, M. I. Sereno, A. M. Dale, *Neuroimage* **9**, 195 (1999); A. M. Dale, B. Fischl, M. I. Sereno, *Neuroimage* **9**, 179 (1999).
9. D. C. Van Essen, H. A. Drury, *J. Neurosci.* **17**, 7079 (1997).
10. M. I. Sereno *et al.*, *Science*, **268**, 889 (1995).
11. N. Hadjikhani, A. K. Liu, A. M. Dale, P. Cavanagh, R. B. Tootell, *Nature Neurosci.* **1**, 235 (1998).
12. M. I. Sereno, *Curr. Opin. Neurobiol.* **8**, 188 (1998).
13. K. Kleist, *Ergeb. Neurol. Psychiatr.* **1**, 342 (1916).
14. M. Critchley, *The Parietal Lobes* (Arnold, London, 1953).
15. J. C. Culham *et al.*, *J. Neurophysiol.* **80**, 2657 (1998).
16. E. Wojciulik, N. Kanwisher, *Neuron* **23**, 747 (1999).
17. R. A. Berman *et al.*, *Hum. Brain Mapp.* **8**, 209 (1999).
18. E. Awh *et al.*, *Psychol. Sci.* **10**, 433 (1999).
19. A. C. Nobre, D. R. Gitelman, E. C. Dias, M. M. Mesulam, *Neuroimage* **11**, 210 (2000).
20. M. Corbetta, J. M. Kincade, J. M. Ollinger, M. P. McAvoy, G. L. Shulman, *Nature Neurosci.* **3**, 292 (2000).
21. J. B. Hopfinger, M. H. Buonocore, G. R. Mangun, *Nature Neurosci.* **3**, 284 (2000).
22. C. L. Colby, J. R. Duhamel, M. E. Goldberg, *J. Neurophysiol.* **76**, 2841 (1996).
23. J. R. Duhamel, F. Bremmer, S. BenHamed, W. Graf, *Nature* **389**, 845 (1997).
24. R. A. Andersen, L. H. Snyder, A. P. Batista, C. A. Buneo, Y. E. Cohen, *Novartis Found. Symp.* **218**, 109 (1998).
25. M. V. Chafee, P. S. Goldman-Rakic, *J. Neurophysiol.* **79**, 2919 (1998).
26. Although LIP neuron activity is strongly modulated by remembered target position, object identity can be important too [A. B. Sereno, J. H. Maunsell, *Nature* **395**, 500 (1998)].
27. G. Wang, M. Tanifuji, K. Tanaka, *Neurosci. Res.* **32**, 33 (1998).
28. A dental impression of each participant was taken outside the magnet. The person's occiput was then supported above the Siemens Small Flex coil with a foam doughnut, padded from the sides with more foam and allowed to settle into position for several minutes. We were careful to avoid any direct contact between the person's inion and the radio frequency (RF) coil. The person's dental impression was then attached to a custom-built dual ball joint plexiglas arm, one end of which was mounted firmly onto the patient tray. The bite-bar end of the arm has three rotational and three translational degrees of freedom, which permits the impression to be moved (within bounds) to any position and angle. This complete positional flexibility is critical in order for a bite bar to provide comfortable positional stability. After participants were satisfied with the bite bar position, it was locked into place. Participants were instructed not to forcibly bite the impression but rather to use it as a reference. This new system provided a marked reduction in motion artifacts in most participants without introducing any discomfort. The participants' direct view of the screen (that is, not via the mirror) was blocked with a horizontal strip of foam mounted near the tip of the nose.
29. S. Funahashi, C. J. Bruce, P. S. Goldman-Rakic, *J. Neurophysiol.* **63**, 814 (1990).
30. In our initial experiments, the dimmed fixation cross was quite dim. However, to avoid the possibility that the dim fixation cross might itself stimulate the retina or be remapped, in later experiments the fixation cross was turned completely off during the saccade to and back from the target. There was no difference between the results obtained in these two variations of the task.
31. Echo-planar images were collected during 512-s runs (1.5-T Siemens Vision, Small Flex quadrature receive-only surface RF coil, single-shot echo planar images, 3 × 3 × 4 mm voxels, 128 images per slice, 24 coronal slices through the occipital and parietal lobes, TE = 42, flip angle = 70°, 64 × 64 matrix, bandwidth = 926 Hz per pixel, eight stimulus cycles). A total of 159 functional scans was performed on 12 participants (108 remembered target scans, 51 scans to map early visual areas, and 487,000 images total). The cortical surface for each participant was reconstructed from a pair of structural scans (1 × 1 × 1 mm MPRAGE sequence) taken in a separate session using a head coil. The last scan of each functional session was an alignment scan (also 1 × 1 × 1 mm MPRAGE) acquired with the surface coil in the plane of the functional scans. The alignment scan was used to establish an initial registration of the functional data with the surface. Additional affine transformations that included a small amount of shear were then applied to the functional scans for each person, using blink comparison with the structural images to achieve an exact overlay of the functional data onto each cortical surface. To increase the signal-to-noise ratio, we typically averaged four 512-s scans for each task. Our functional data did not extend significantly into the frontal lobe, and so we cannot say whether frontal areas were activated by our paradigm. The software used for all stages of this process (FreeSurfer) is available for free download (binaries for IRIX and Linux) at http://surfer.nmr.mgh.harvard.edu/download.html.
32. A similarly positioned bilateral parietal focus appears in most of the attention studies cited in (*15–21*); see also figure 2 from the spatial attention study of A. Martinez *et al.* [*Nature Neurosci.* **2**, 364 (1999)],

which illustrates a similar posterior parietal focus ("par.") in flat maps. We used the Montreal Neurological Institute Automated Linear Registration Package [described in D. L. Collins, P. Neelin, T. M. Peters, A. C. Evans, *J. Comp. Assist. Tomogr.* **18**, 192 (1994) and available for free download at ftp://ftp.bic.mni.mcgill.ca/pub/mni_autoreg/] to generate Talairach transformation matrices. We measured the average Talairach coordinates of the center of the parietal focus in the right hemisphere across $n = 22$ scan sessions ($n = 12$ unique participants) (Talairach coordinates were as follows: $x = 24$ mm, $y = -65$ mm, $z = 53$ mm; SD: $x = 6$ mm, $y = 5$ mm, $z = 6$ mm).

33. Data from both phase-encoded and two-condition experiments were initially analyzed by a fast Fourier transform on the brightness time course from each voxel. Statistical significance was calculated and displayed by converting the Fourier magnitude of the response to an *F* statistic. When color (red, blue, or green) is used to represent phase, the significance controls the saturation; when color is used to represent significance (red-orange or blue-cyan), the phases are collapsed into two bins (that is, contralateral/ipsilateral and ON/OFF). The minimal regions of the ipsilateral phase (for example, small blue spots in the *F*-statistic map in Fig. 3, upper right) have been suppressed in the phase maps (compare the images in Fig. 3, upper left and upper right pairs). The exceptional systematicity of the parietal maps is best appreciated in an animation where each response phase contour is successively marked with a white stripe. Mpeg movies posted at http://kamares.ucsd.edu/~sereno/LIP/ show the response of the left hemisphere (lefthemi.mpg) and the right hemisphere (righthemi.mpg) to one complete target-angle cycle in task 1 on a medial-posterior view of the inflated cortical surface. The relation between the left and right hemisphere responses is illustrated in a closeup movie of the left and right parietal foci (bothcloseup+stim.mpg) that also includes a representation of the corresponding location of the target. In all movies, ipsilateral phases have not been truncated. A small amount of bilateral activation is visible in the closeup movie as the stimulus crosses the upper and lower vertical meridians.
34. M. I. Sereno, S. Pitzalis, A. Martinez, data not shown.
35. Human V3A was originally defined as a thick strip of retinotopic (non–mirror image) cortex directly anterior to lower field–only V3 that contains upper as well as lower fields [R. B. Tootell *et al.*, *J. Neurosci.* **17**, 7060 (1997)]. Although the names "V3" and "V3A" were taken from macaque monkeys, the functional and anatomical properties of the human areas differ from their macaque monkey namesakes. The strong response to motion and the heavy myelination of human V3A [see figure 5 in M. I. Sereno, J. M. Allman, in *The Neural Basis of Visual Function*, A. Leventhal, Ed. (Macmillan, London, 1991), pp. 160–172, and figure 8 in R. B. H. Tootell, J. B. Taylor, *Cereb. Cortex* 1995, **5**, 39 (1995): labeled "possible/presumptive MT" in both instances] recall the direction selectivity and myelination of lower field–only macaque monkey V3 rather than macaque monkey V3A. Owl monkeys also have a dorsal, heavily myelinated, direction-selective area, DM [J. M. Allman, J. H. Kaas, *Brain Res.* **100**, 473 (1975)], that contains upper and lower fields like human V3A; but owl monkey DM directly adjoins V2—like macaque V3 but unlike human V3A [see (*5*, *12*) for comparison maps]. Different authors have subsequently published tentative and partly conflicting subdivisions of this region in humans [A. T. Smith, M. W. Greenlee, K. R. Singh, F. M. Kraemer, J. Hennig, *J. Neurosci.* **18**, 3816 (1998); R. B. Tootell *et al.*, *Neuron* **21**, 1409 (1998); W. A. Press, A. A. Brewer, R. F. Dougherty, A. R. Wade, B. A. Wandell, *Vis. Res.* **41**, 1321 (2001); R. B. Tootell, N. Hadjikhani, *Cereb. Cortex* **11**, 298 (2001)]. To summarize, with a large V3A as a starting point, V3B is directly inferior to V3A, V7 is anterior to both V3A and V3B, and a two-part lateral occipital area in the expected location of V4d overlaps V3B completely. We are confident that our posterior focus overlaps the superior half of V3A and V7 but not V3B or the lateral occipital areas, and we are sure that our parietal focus lies completely anterior and superior to V7.
36. It is likely that the distractors also served as an (unbiased) probe of the attended-to region. Single-unit recording experiments in the macaque monkey LIP (*22–24*) have shown that when an animal is attending to a particular location, neurons with receptive fields at that location give an enhanced response to a probe stimulus there; a response that typically greatly exceeds the activity attributable to mere attention to that location on a blank screen.
37. Although peripheral attention is not necessary in standard phase-encoded retinotopic mapping experiments (the only task is continuous central fixation), it is unlikely that attention to the periphery can be completely suppressed. Maps derived from standard retinotopic mapping experiments therefore probably reflect a mix of "sensory" retinotopy and "attentional" retinotopy and also a different mix in different areas. With our task, there were weaker but significant responses in early retinotopic areas (V1, V2, V3, and VP) that were retinotopically consistent in polar angle; that is, upper field (= red+blue) inferiorly and lower field (= green+blue) superiorly, and at the expected location in the eccentricity map. We set our significance thresholds conservatively (a steep sigmoidal function for the mapping between significance and color saturation); with a somewhat more lax criterion, these spotty responses at (just) the eccentricity corresponding to the target in V1/V2/V3/VP become filled in.
38. In the parietal as well as the prefrontal cortex, most neurons signal the location of the target, even when the animal makes an anti-saccade [S. Funahashi, M. V. Chafee, P. S. Goldman-Rakic, *Nature* **365**, 753 (1993); J. Gottlieb, M. E. Goldberg, *Nature Neurosci.* **2**, 906 (1999)].
39. The orientation of the visual field map reported here (upper → anterior, lower → posterior) is roughly similar (once the cortex has been unfolded) to what was found in a mapping study of the LIP in anesthetized macaques [G. J. Blatt, R. A. Andersen, G. R. Stoner, *J. Comp. Neurol.* **299**, 421 (1990); we made a surface reconstruction from the data shown in their figure 5]. One difference already noted is that the human area sits in a small sulcus slightly medial and posterior to the intraparietal sulcus instead of inside it. This recalls the situation with human MT, which typically sits in a small sulcus just posterior and ventral to the superior temporal sulcus instead of inside it, on its posterior bank. Finally, it has long been known that human V1 doesn't extend as far onto the lateral surface as it does in other primates. In each case, the presumed human homolog has moved radially outward (superiorly, posteriorly, and inferiorly) from the center of the lateral surface of the occipital lobe.
40. Retinotopically organized delay-period activity has been observed in a number of different brain structures in many different vertebrates. In monkeys, but also in frogs, a briefly presented stimulus can elicit retinotopically localized activity in the superior colliculus that persists over many seconds [D. Ingle, *Science* **188**, 1033 (1975); L. E. Mays, D. L. Sparks, *J. Neurophysiol.* **43**, 207 (1980); P. W. Glimcher, D. L. Sparks, *Nature* **355**, 542 (1992)].
41. We thank R. Buxton, E. Wong, and L. Frank for their generosity with scan time, pulse sequences, and advice; C. Kemper for help with scanning; A. Dale for motion and retinotopic mapping stimulus code; E. Awh, G. Boynton, A. Dale, B. Fischl, C. Fernety, M. Kutas, S. Hillyard, A. Liu, and E. Vogel for help and discussions; and G. Boynton for the use of his projection screen and frame. Supported by the Human Frontier Science program (E. Halgren), NIH grant NICHD22614 (M. Kutas), Office of Naval Research grant N00014-93-0942 (S. Hillyard), and NIMH grant MH25594 (A.M.).

22 June 2001; accepted 10 September 2001

CNS Synaptogenesis Promoted by Glia-Derived Cholesterol

Daniela H. Mauch,[1] Karl Nägler,[1,3] Stefan Schumacher,[4] Christian Göritz,[1,3] Eva-Christina Müller,[2] Albrecht Otto,[2] Frank W. Pfrieger[1,3]*

The molecular mechanisms controlling synaptogenesis in the central nervous system (CNS) are poorly understood. Previous reports showed that a glia-derived factor strongly promotes synapse development in cultures of purified CNS neurons. Here, we identify this factor as cholesterol complexed to apolipoprotein E–containing lipoproteins. CNS neurons produce enough cholesterol to survive and grow, but the formation of numerous mature synapses demands additional amounts that must be provided by glia. Thus, the availability of cholesterol appears to limit synapse development. This may explain the delayed onset of CNS synaptogenesis after glia differentiation and neurobehavioral manifestations of defects in cholesterol or lipoprotein homeostasis.

The formation of synaptic contacts is a critical phase during brain development and plays a crucial role in long-term synaptic plasticity in the adult CNS, but the cell biological mechanisms that mediate the assembly of the synaptic machinery are still poorly understood. A possible role of glial cells in CNS synaptogenesis was indicated by a series of studies (*1–3*) on rat retinal ganglion cells (RGCs), CNS neurons that can be highly purified (*4*) and cultured under defined glia-free conditions (*5*). The previous reports (*1–3*) showed that neurons formed few and inefficient synapses in the absence of glia and that glial cells induced the formation of numerous and highly efficient synapses without affecting neuronal survival, excitability, or

[1]Synapse Group and [2]Protein Chemistry Group, Max-Delbrück-Center for Molecular Medicine, D-13092 Berlin, Germany. [3]Max-Planck/CNRS Group, UPR 2396, Centre de Neurochimie, F-67084 Strasbourg, France. [4]Institute for Cell Biochemistry and Clinical Neurobiology, University of Hamburg, D-20246 Hamburg, Germany.

*To whom correspondence should be addressed. E-mail: fw-pfrieger@gmx.de